molecular pharmaceutics

pubs.acs.org/molecularpharmaceutics

Article

Lipid Nanoparticle Delivery of iMDK Induces ATF3-Mediated Apoptosis in Sotorasib-Resistant KRAS Mutant Lung Cancer

Bingxin Liu, Iris M. Fink-Baldauf, William D. Stuart, Cheng Jiang, Anjaparavanda P. Naren, Donglu Shi, Minzhe Guo, Jeffrey A. Whitsett, and Yutaka Maeda*

Cite This: https://doi.org/10.1021/acs.molpharmaceut.5c00550

Read Online

ACCESS | Metrics & More | Article Recommendations | Supporting Information

ABSTRACT: The small molecule iMDK induces apoptosis in H441 papillary lung adenocarcinoma cells that harbor $KRAS^{G12V}$; however, the molecular mechanism by which iMDK induces apoptosis remains unknown. In addition, due to its hydrophobic structure, iMDK is insoluble in water, making iMDK unsuitable for clinical translation. To understand the molecular mechanism, we conducted RNA-seq analysis to identify genes that are regulated by iMDK in H441 cells. RNA-seq data analysis indicated that iMDK activated the ATF3-CHOP (DDIT3)-mediated apoptotic pathway. iMDK did not induce apoptosis in ATF3 or CHOP CRISPR knockout H441 cells, indicating that iMDK induced apoptosis through the ATF3-CHOP pathway. Notably, iMDK also activated ATF3 and induced apoptosis in both sotorasib ($KRAS^{G12C}$ inhibitor)-naïve and resistant H358 bronchioalveolar carcinoma cells that harbor $KRAS^{G12C}$. To administer iMDK in water, we encapsulated iMDK in multiple lipid or polymer nanoparticles that could be suspended in water. Importantly, iMDK that was encapsulated in DPPC/DOTAP/DSPE-PEG/Cholesterol lipid nanoparticles but not DPPC/DPPG/DSPE-PEG/Cholesterol or PEI−PEG-LinA nanoparticles induced apoptosis in H441 cells in vitro. Intraperitoneal injection of water-soluble iMDK lipid nanoparticles (DPPC/DOTAP/DSPE-PEG/Cholesterol) significantly reduced the growth of H441 xenografts without inducing liver toxicity in vivo. These results suggest that water-soluble iMDK lipid nanoparticle delivery is effective for treating subtypes of KRAS mutant lung cancers that retain the ATF3-mediated apoptotic pathway.

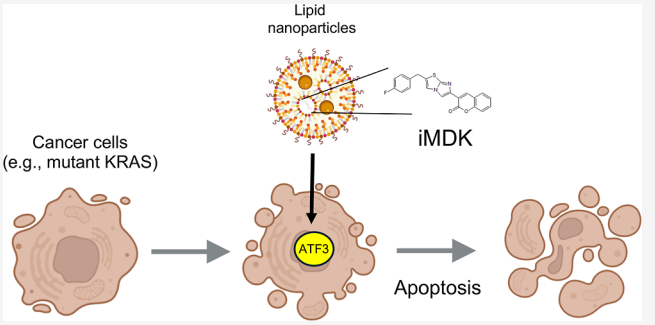

KEYWORDS: *LNP, iMDK, ATF3, CHOP, KRAS, lung cancer*

INTRODUCTION

iMDK (3-[2-[(4-Fluorophenyl)methyl]imidazo[2,1-*b*]thiazol-6-yl]-2*H*-1-benzopyran-2-one) (Figure 1a) was originally discovered as a small molecule that inhibits the expression of MDK (also known as midkine), a growth factor that is expressed in H441 human lung papillary adenocarcinoma cells that carry the driver oncogene $KRAS^{G12V}$.[1] Molecular and biochemical analyses indicated that iMDK also inhibited the PI3K-AKT pathway and induced apoptosis in H441 cells, HEK293 human embryonic kidney cells, and H520 human lung squamous cell carcinoma cells but not A549 human lung carcinoma cells that carry $KRAS^{G12S}$ or NHLF normal human lung fibroblasts.[1] iMDK has also been shown to effectively suppress growth of HSC-2 human oral squamous carcinoma cells,[2] PC3 human prostate cancer cells,[3] H1299 human nonsmall cell lung carcinoma cells,[4] BCBL-1, BC-1, GTD, TY-1 primary effusion lymphoma cells,[5] and KMM-1, NCI-H929, and RPMI-8226 multiple myeloma cells.[6] Although iMDK is potentially a promising cancer drug to suppress the growth of subtypes of cancer cells, the molecular mechanism by which iMDK suppresses cancer cell growth remains unknown. Also, the insolubility of iMDK in water due to its hydrophobicity hampers efforts to translate iMDK into the clinic. Previous in vitro and in vivo xenograft studies were conducted by dissolving iMDK into the toxic solvent DMSO,[1,2,7] which is not suitable for preclinical and clinical application.

In the present study, to understand the molecular mechanism by which iMDK induces apoptosis in H441 lung cancer cells carrying $KRAS^{G12V}$, we conducted RNA-seq combined with a gene knockout approach using CRISPR/Cas9 and aimed to identify genes that are involved in apoptosis induced by iMDK. The recent discovery of small molecules (e.g., sotorasib) that bind to $KRAS^{G12C}$ and in turn suppress the growth of cancer cells that are driven by $KRAS^{G12C}$ has revolutionized the treatment strategy for KRAS mutant lung

Received: April 16, 2025
Revised: July 24, 2025
Accepted: July 25, 2025

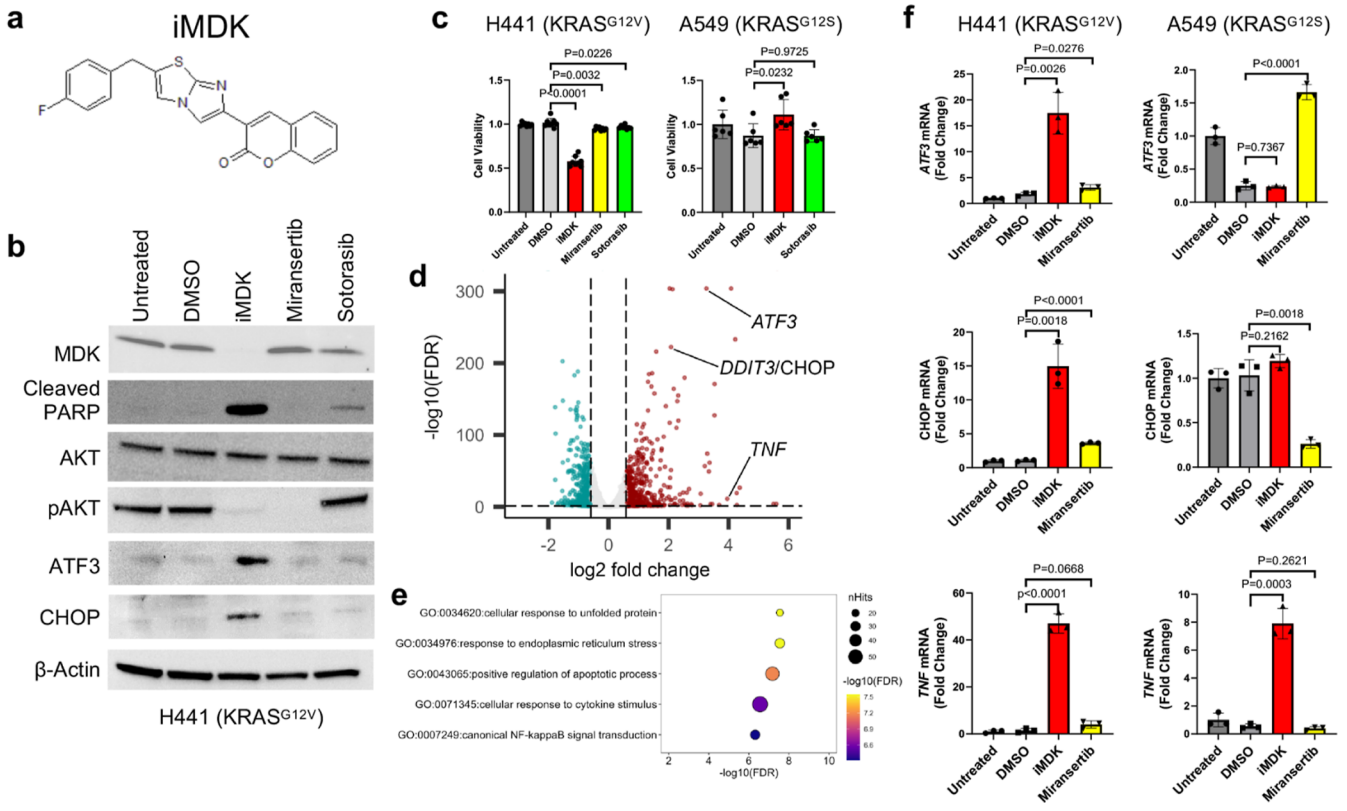

Figure 1. iMDK induces the expression of ATF3 and DDIT3 (also known as CHOP) in H441 papillary lung adenocarcinoma cells that harbor $KRAS^{G12V}$. (a) Structure of iMDK. (b) Immunoblots indicating the expression of proteins from cell extracts of H441 cells that were treated with DMSO, iMDK (5 μM), miransertib (10 μM), and sotorasib (10 μM) for 48 h. (c) Cell viability measured by the MTS assay for H441 and A549 lung carcinoma cells ($KRAS^{G12S}$) that were treated with DMSO, iMDK (5 μM), miransertib (10 μM), and sotorasib (10 μM) for 48 h (n = 8). (d) Volcano plot of DESeq2 tests for genes that are differentially expressed (fold change ≥1.5 and adjusted P value < 0.1) from RNA-seq of H441 cells treated with iMDK (5 μM) vs DMSO for 24 h. (e) Gene ontologies associated with genes significantly upregulated in H441 cells treated with iMDK that were analyzed in (d). (f) TaqMan gene expression analysis indicating mRNA expression of *ATF3*, CHOP (*DDIT3*), and *TNF* from H441 and A549 cells that were treated with DMSO, iMDK (5 μM), or miransertib (10 μM) for 24 h (n = 3). Student's t-test values are indicated above bars. Error bars represent ± standard deviation.

cancers; however, such cancer cells eventually become resistant to $KRAS^{G12C}$ inhibitors by different mechanisms,[8,9] thus urging the cancer research community to develop novel therapeutics to treat such $KRAS^{G12C}$ inhibitor-resistant cancers. We sought to determine whether iMDK can suppress the growth of sotorasib-resistant H358 bronchioalveolar carcinoma cells that harbor $KRAS^{G12C}$. Additionally, to aid future clinical application, we developed a water-soluble form of iMDK using lipid nanoparticle (LNP) technology to encapsulate iMDK, which can then be dissolved in water instead of DMSO.

MATERIALS AND METHODS

Materials. Lipids were purchased from Avanti Polar Lipids (Alabaster, AL, USA), including 18:1 TAP (DOTAP) (cat#: 890890), 16:0 PC (DPPC) (cat#: 850355), and 16:0 PG (DPPG) (cat#: 840455). *O*-Methyl-*O*′-succinylpolyethylene glycol 2′000 (cat#: 17928), poly(ethylenimine) solution (cat#: 408700), linoleic acid (cat#: L1376), and the ALT Activity Assay (cat#: MAK052) were purchased from MilliporeSigma (St. Louis, MO, USA). EDC (cat#: 22981) and *N*-hydroxysuccinimide (NHS) (cat#: 24500) were purchased from Thermo Fisher (Waltham, MA, USA). iMDK (cat#: 5126) and sotorasib (also known as AMG510; cat#: 7713) were purchased from Tocris Bioscience (Minneapolis, MN, USA). Miransertib (also known as ARQ092; cat#: HY-19719) was purchased from MedChemExpress (Monmouth Junction, NJ, USA).

Cells. H441 papillary lung adenocarcinoma cells, A549 lung carcinoma cells, and H358 bronchioalveolar carcinoma cells were obtained from ATCC (Manassas, VA, USA). H358R cells (sotorasib-resistant H358 cells) were generated by culturing H358 cells at 10 μM sotorasib for 8 months. ATF3 or CHOP (DDIT3) knockout H441 cells were created using ATF3 CRISPR Plasmids (h) (cat#: sc-416577, Santa Cruz Biotechnology, Dallas, TX, USA) or DDIT3/CHOP/GADD153 CRISPR Plasmids (h) (cat#: sc-400051-KO-2, Santa Cruz Biotechnology).

Immunoblot Analysis. Cells were lysed in ice-cold RIPA Lysis and Extraction Buffer (cat#: PI89900; Thermo Fisher). Cell lysates were cleared by centrifugation (30 min at 10,000g at 4 °C), and protein concentration was determined using Direct Detect Assay-free Cards (cat#: DDAC00010-GR; MilliporeSigma). Equal amounts of protein (50 μg) were separated on an SDS-PAGE gel. The gel was electrophoretically transferred to a Hybond PVDF transfer membrane and incubated with primary and secondary antibodies. An antibody specific for actin (cat#: LMAB-C4) was obtained from Seven Hills Bioreagents (Cincinnati, OH, USA). An antibody specific for MDK (also known as midkine) was obtained from Abcam (cat#: ab52637, Waltham, MA, USA). Antibodies specific for

https://doi.org/10.1021/acs.molpharmaceut.5c00550
Mol. Pharmaceutics XXXX, XXX, XXX−XXX

P-AKT (cat#: 4060S), AKT (cat#: 9272S), Cleaved PARP (cat#: 5625S), P-ERK (MAPK T202/Y204, cat#: 9101S), ERK1/2 (cat#: 4695S), CHOP (cat#: 2895S), and ATF3 (cat#: 18665S) were obtained from Cell Signaling Technology (Danvers, MA, USA).

Cell Viability Assay. Cells were plated in 24-well plates at a density of 1×10^5 cells and cultured at 37 °C for 24 h. Medium was removed by aspiration and replaced with fresh culture medium containing iMDK (5 μM), miransertib (10 μM), or sotorasib (10 μM) that was dissolved in DMSO or iMDK that was encapsulated in water-soluble nanoparticles. Cells were treated for 48 h before an MTS assay to determine cell viability based on the manufacturer's protocol (CellTiter 96 AQ Cell proliferation assay, cat#: G3582; Promega, Madison, WI, USA).

RNA-Seq Analysis. For RNA-seq, RNA was extracted from H441 cells treated with DMSO or iMDK at 5 μM for 24 h. RNA was sent to the CCHMC DNA sequencing core (Cincinnati, OH, USA) as described previously.[10] Quality assessment and preprocessing of RNA-seq reads were performed using FASTQC, Trim Galore, and SAMtools. Reads were then aligned to the hg38 genome using Bowtie2. Low-quality alignments were removed by using SAMtools. Potential PCR duplication reads were identified using the Picard tool and excluded. Gene expression was counted using htseq-count. Differential expression analysis was performed using the Bioconductor DESeq2 package.[11] Differential expression with at least a 1.5-fold change and false discovery rate <0.1 was considered significant. A volcano plot showing the differential expression result was generated using the Bioconductor EnhancedVolcano package. Gene ontology (GO) analysis was conducted using the ToppGene Suite bioinformatical tool (https://toppgene.cchmc.org).[12]

qRT-PCR. RNA was extracted from H441, H358, and A549 cells using the QIAGEN RNeasy Mini Kit (cat#: 74104; QIAGEN, Germantown, MD, USA). Following extraction, reverse transcription reactions were carried out with an iScript cDNA synthesis kit (cat#: 1708890; Bio-Rad, Hercules, CA, USA) according to the provided manufacturer's instructions. The synthesized cDNA was used for quantitative PCR (qPCR) using a StepOnePlus Real-Time PCR System with specific TaqMan gene expression assay probes for *ATF3* (cat#: 4331182; Hs00231069_m1), CHOP (also known as *DDIT3*; cat#: 4331182; Hs00358796_g1), *TNF* (cat#: 4331182; Hs00174128_m1), and 18S RNA (cat#: 4333760T) (Thermo Fisher). Expression levels of *ATF3*, CHOP (*DDIT3*), and *TNF* were normalized using 18S RNA to control for variations in RNA input and cDNA synthesis efficiency. The resultant data were expressed as mean ± standard deviation (SD) and analyzed statistically using the 2-tailed Student's *t*-test to determine significance. All statistical analyses were conducted using GraphPad Prism version 10 (GraphPad Software, Boston, MA, USA).

Nanoparticle Formulation. DPPC/DOTAP/DSPE-PEG/Cholesterol (DPPC[DOTAP]) or DPPC/DPPG/DSPE-PEG/Cholesterol (DPPC[DPPG]) was dissolved in chloroform at concentrations of 25, 12.5, 12.5, and 5 mg/mL, respectively. Each lipid preparation (3 mL) was mixed thoroughly in a round-bottom flask. The organic solvent was then removed by using a rotary evaporator to form a thin lipid film on the walls of the flask. The lipid film was hydrated with 16.5 mL of deionized (DI) water to form liposomes at a final concentration of 10 mg/mL. The liposome suspension was put into a sonicator water bath for 2 h at room temperature to reduce the particle size and ensure uniformity. The liposome solution was transferred to a 50 mL tube and subjected to additional water bath sonication. While maintaining sonication, 6.6 mL of iMDK dissolved in tetrahydrofuran (THF) at a concentration of 5 mg/mL was added dropwise to the liposome suspension. After the addition was complete, the mixture was sonicated for another 30 min. The iMDK-loaded lipid nanoparticle (LNP) solution was then transferred back to the round-bottom flask, and THF was removed by using rotary evaporation. To purify the iMDK-loaded LNPs, the solution was dialyzed against DI water for 6 h to remove any remaining THF and unencapsulated iMDK. The final iMDK LNP solution was then ready for use. Before each use, the iMDK LNPs were sonicated for an additional 30 min to ensure quality.

For PEI−PEG-LinA synthesis, polyethylenimine (PEI) was functionalized with biological fatty acids and polyethylene glycol (PEG) via amidation using EDC/NHS-mediated coupling, following a standard reaction scheme for all coupling reactions as we previously described.[13] Briefly, 450 mg (0.25 mmol) of PEI (MW 1800) was dissolved in 15 mL of ethanol at 40°C for 15 min. Next, 150 mg (0.075 mmol) of PEG-COOH, 350 mg (1.250 mmol) of LinA, 316 mg (1.656 mmol) of EDC, and 238 mg (2.070 mmol) of NHS were dissolved in 15.75 mL of ethanol plus 1.57 mL of 500 mM MES buffer and reacted at 40 °C for 15 min. The two solutions were immediately mixed and allowed to react overnight at 40 °C. After the reaction, ethanol was removed via rotary evaporation, and the product was resuspended in deionized water. The conjugated PEI was dialyzed against deionized water using a 20 kDa membrane for 4−5 days, extracted twice with diethyl ether, and lyophilized. Before use, the lyophilized polymers were suspended in 10 mM MOPS buffer (pH 7.4) and sonicated.

Mouse Experiments. All animal experiments conducted were approved by the Cincinnati Children's Hospital Institutional Animal Care and Use Committee (IACUC) under protocol 2023-0034, which is amended and reviewed yearly. Human H441 lung cancer xenografts were established in 6−8 wk-old female NU/J nude mice (cat#: 002019; Jackson Laboratory, Bar Harbor, ME, USA) by subcutaneous (s.c.) injection of H441 cells (1×10^6/50 μL) mixed with Matrigel (cat#: CB-40234A; BD Pharmingen, San Diego, CA, USA) into the dorsal flank. The mice were randomly assigned into three groups (n = 8 per group) 5−8 days after tumor inoculations. iMDK (9.7 mg/kg) dissolved in 100% DMSO (iMDK-DMSO) or formulated in LNP (iMDK-LNP) was intraperitoneally injected every day. Tumors were measured 5, 10, and 13 days after the first injection of iMDK, and the tumor volume was calculated as $a \times b^2 \times 0.5$, where a and b were large and small diameters, respectively. After treatment for 13 days, body weights were measured and mice were euthanized. Xenografts were then removed and prepared for histological analyses. For the analysis of serum ALT, blood was drawn from the heart of the mice 13 days after the first iMDK injection.

RESULTS

RNA-Seq Indicating that iMDK Activates the ATF3-CHOP-Mediated Apoptotic Pathway. We previously identified small molecule iMDK as an inhibitor of the expression of MDK and an inducer of apoptosis in H441

https://doi.org/10.1021/acs.molpharmaceut.5c00550
Mol. Pharmaceutics XXXX, XXX, XXX−XXX

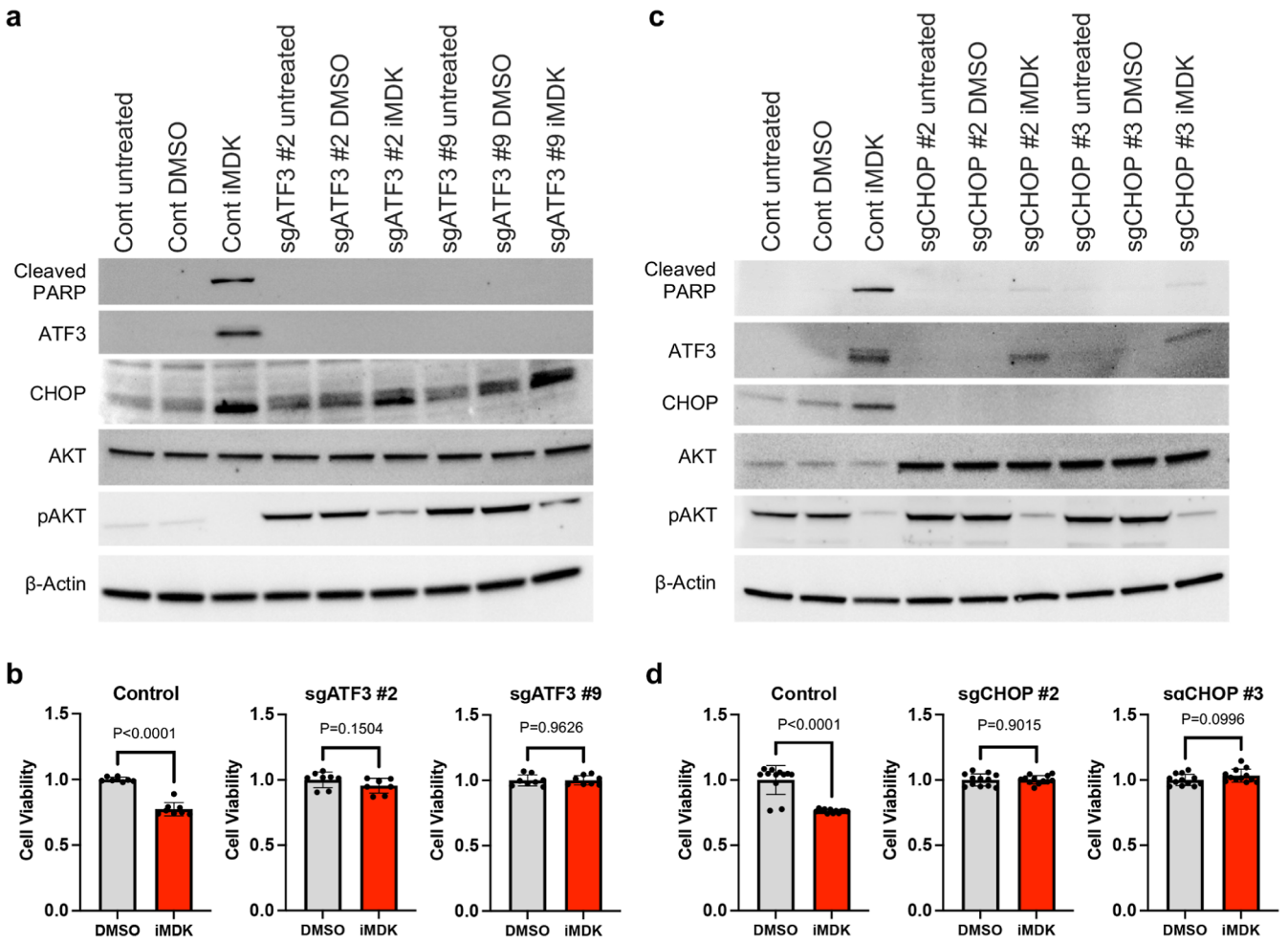

Figure 2. ATF3 and CHOP are required for iMDK-mediated apoptosis in H441 cells. (a) Immunoblots indicating the expression of proteins from H441 cell extracts with or without ATF3 (CRISPR/Cas9 with sgATF3 #2 or #9) that were treated with DMSO or iMDK (0.5 μM) for 48 h. (b) Cell viability measured by MTS assay for H441 cells with or without ATF3 (CRISPR/Cas9 with sgATF3 #2 or #9) that were treated with DMSO or iMDK (0.5 μM) for 48 h (n = 8). (c) Immunoblots indicating that cleaved PARP was induced by iMDK in H441 control cells but not in H441 cells lacking CHOP (CRISPR/Cas9 with sgCHOP #2 or #3). (d) Cell viability measured by the MTS assay for H441 cells with or without CHOP (sgCHOP #2 or #3) that were treated with DMSO or iMDK (0.5 μM) for 48 h (n = 12). Student's t-test values are indicated above bars. Error bars represent ± standard deviation.

papillary lung adenocarcinoma cells that harbor $KRAS^{G12V}$ (Figure 1b,c).[1] Since we also identified that iMDK inhibited the PI3K-AKT pathway in H441 cells[1] (Figure 1b), we hypothesized that iMDK induces apoptosis through the inhibition of the PI3K-AKT pathway. However, miransertib (also known as ARQ092),[14] another PI3K-AKT pathway inhibitor, inhibited the PI3K-AKT pathway in H441 cells but failed to induce PARP cleavage, a marker for apoptosis (Figure 1b), and failed to suppress cell growth (Figure 1c), indicating that the inhibition of the PI3K-AKT pathway is not sufficient to explain the mechanism by which iMDK induced apoptosis in H441 cells. To identify the mechanism, we sought to determine the genes that were affected by iMDK in an unbiased fashion using RNA-seq with RNA isolated from H441 cells that were treated with iMDK or DMSO (control) for 24 h. RNA-seq analysis indicated that iMDK significantly induced 545 genes while reducing 491 genes (fold change ≥1.5 and adjusted P value <0.1; Figure 1d and Table S1). We analyzed the 545 genes induced by iMDK using the ToppGene Suite bioinformatical tool (https://toppgene.cchmc.org),[12] which indicated that 48 genes fall into the positive regulation of the apoptotic process (GO: 0043065) (Figure 1e and Table S2). Among the 48 genes, *ATF3*, *DDIT3* (also known as CHOP; hereafter, CHOP), and *TNF* are of particular interest since the ATF3-CHOP endoplasmic reticulum (ER) stress pathway,[15−17] and TNF[18] are known to induce apoptosis in specific cell types. The induction of ATF3, CHOP, and TNF by iMDK in H441 cells was confirmed by TaqMan gene expression analysis and Western blotting (Figure 1b,f). Of note, miransertib neither induced the expression of ATF3 nor CHOP (Figure 1b,f), indicating that the PI3K-AKT pathway does not mediate the induction of ATF3 and CHOP by iMDK. Previously, we showed that iMDK did not induce apoptosis in A549 lung carcinoma cells that harbor $KRAS^{G12S}$ (Figure 1c).[1] We assessed the expression of *ATF3*, CHOP, and *TNF* in A549 cells treated with iMDK. Notably, iMDK induced the expression of *TNF* but not *ATF3* or CHOP in A549 cells (Figure 1f), suggesting that the induction of *ATF3* and CHOP but not *TNF* by iMDK is required for iMDK-mediated induction of apoptosis in H441 cells.

ATF3-CHOP Pathway Being Required for the Apoptosis Induced by iMDK in H441 Cells. To determine the

https://doi.org/10.1021/acs.molpharmaceut.5c00550
Mol. Pharmaceutics XXXX, XXX, XXX−XXX

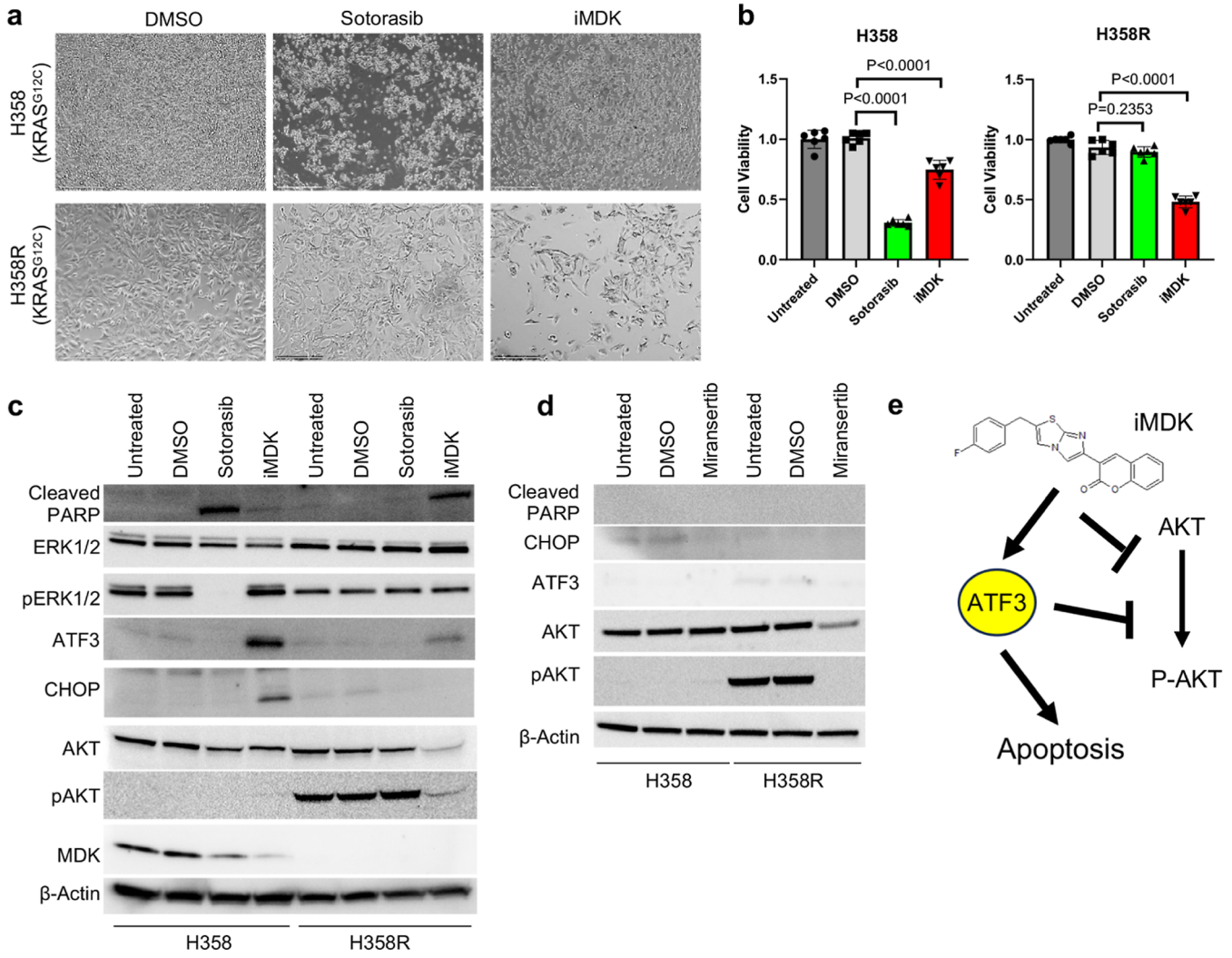

Figure 3. iMDK suppressed the growth of KRAS^{G12C} inhibitor (sotorasib)-resistant H358 cells (H358R) carrying KRAS^{G12C}. (a) Phase contrast images showing H358 and H358R cells that were treated with DMSO, sotorasib (10 μM) or iMDK (5 μM) for 48 h. (b) Cell viability measured by MTS assay for H358 and H358R cells that were treated with DMSO, sotorasib (10 μM) or iMDK (5 μM) for 48 h (n = 6). (c) Immunoblots indicating the expression of proteins from cell extracts of H358 and H358R cells that were treated with DMSO, sotorasib (10 μM) or iMDK (5 μM) for 48 h. (d) Immunoblots indicating the expression of proteins from cell extracts of H358 and H358R cells that were treated with DMSO or miransertib (10 μM) for 48 h. (e) Proposed mechanism by which iMDK induces apoptosis through induction of ATF3. Student's t-test values are indicated above bars. Error bars represent ± standard deviation.

role of the ATF3-CHOP pathway in iMDK-mediated apoptosis in H441 cells, we used the CRISPR/Cas9 genome editor to knock out ATF3 or CHOP in H441 cells and assessed the apoptotic effect of iMDK in the knockout cells. Notably, iMDK induced cleaved PARP and reduced cell growth in parent H441 cells but not in ATF3 knockout H441 cells (two independent clones #2 and #9) (Figure 2a,b), indicating that iMDK requires ATF3 to induce apoptosis in H441 cells. Likewise, iMDK failed to induce cleaved PARP and reduce cell growth in CHOP knockout H441 cells (two independent clones #2 and #3; Figure 2c,d), indicating that iMDK also requires CHOP to induce apoptosis in H441 cells. These data indicate that iMDK induces apoptosis in H441 cells through induction of the ATF3-CHOP pathway.

iMDK Inducing Apoptosis in KRAS^{G12C} Inhibitor (sotorasib)-Naïve and Resistant H358 Bronchioalveolar Carcinoma Cells that Harbor KRAS^{G12C}. Sotorasib (also known as AMG510) has recently been approved[19] by the FDA to treat nonsmall cell lung cancer (NSCLC) that harbors KRAS^{G12C}; however, the majority of the sotorasib-treated NSCLC recurs even after an initial successful response; therefore, new therapeutics are required to target such sotorasib-resistant NSCLC. We hypothesized that iMDK might suppress the growth of sotorasib-resistant NSCLC. We created sotorasib-resistant H358 bronchioalveolar carcinoma cells that harbor KRAS^{G12C} by culturing the cells long-term with sotorasib at 10 μM for 8 months (hereafter, H358R cells). We treated parent H358 and H358R cells with sotorasib or iMDK and assessed the cell growth. As expected, sotorasib significantly suppressed the growth of H358 cells (Figure 3a,b) associated with the induction of cleaved PARP and inhibition of pERK (Figure 3c) but did not suppress the growth of H358R cells (Figure 3a,b). iMDK also significantly suppressed the growth of H358 cells (Figure 3a,b) associated with induction of cleaved PARP, ATF3, and CHOP though less effectively than sotorasib (of note, the expression of pAKT was low in H358 cells) (Figure 3c). Importantly, iMDK significantly suppressed the growth of H358R cells (Figure

https://doi.org/10.1021/acs.molpharmaceut.5c00550
Mol. Pharmaceutics XXXX, XXX, XXX−XXX

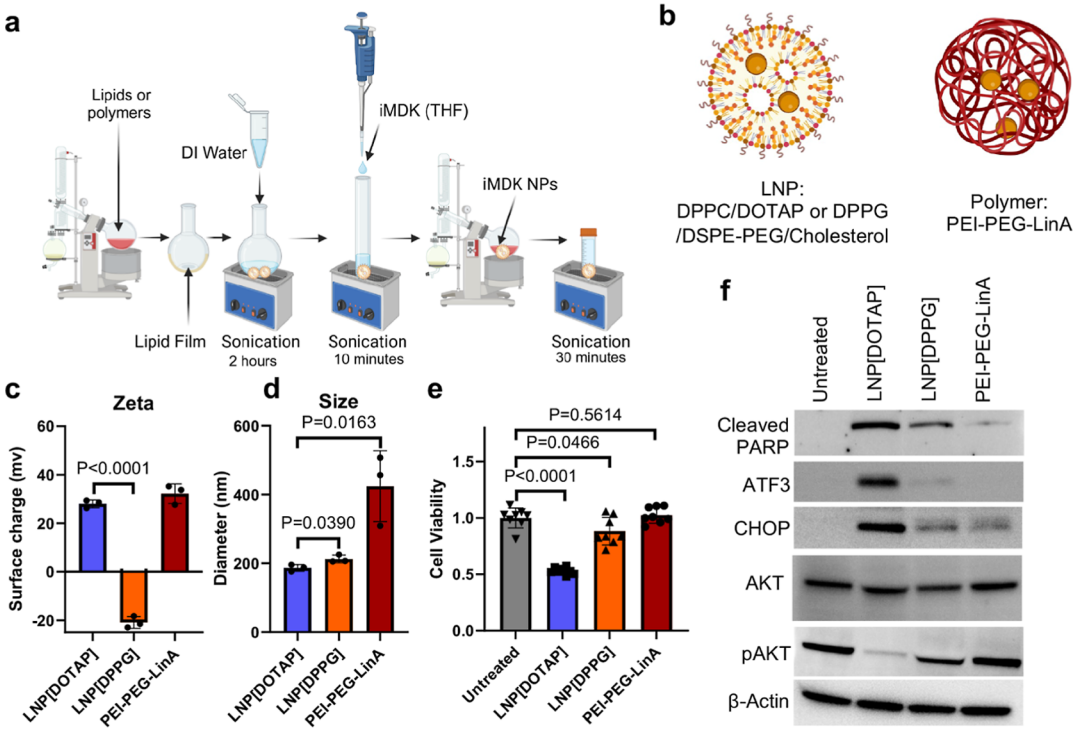

Figure 4. Lipid nanoparticles (LNP; DPPC/DOTAP/DSPE-PEG/Cholesterol) carrying iMDK induce apoptosis in H441 cells in vitro. (a) Experimental scheme synthesizing LNP carrying iMDK. (b) Structure of lipid (left) or PEI (right) nanoparticles. (c) Zeta potential of DPPC/DOTAP/DSPE-PEG/Cholesterol (hereafter, LNP[DOTAP]), DPPC/DPPG/DSPE-PEG/Cholesterol (hereafter, LNP[DPPG]), and PEI−PEG-LinA that carry iMDK (n = 3). (d) Hydrodynamic diameters (size) of LNP[DOTAP], LNP[DPPG], and PEI−PEG-LinA that carry iMDK (n = 3). (e) Cell viability measured by MTS assay for H441 cells that were treated with LNP[DOTAP], LNP[DPPG], and PEI−PEG-LinA that carry iMDK estimated at 5 μM for 48 h (n = 8). (f) Immunoblots indicating the expression of proteins from cell extracts of H441 cells that were treated with LNP[DOTAP], LNP[DPPG], and PEI−PEG-LinA that carry iMDK estimated at 5 μM for 48 h. Panels a and b were made with BioRender.com. Student's t-test values are indicated above bars. Error bars represent ± standard deviation.

3a,b) associated with the induction of cleaved PARP and ATF3 (but not CHOP) as well as the inhibition of AKT (Figure 3c). Miransertib, a PI3K-AKT pathway inhibitor, failed to induce cleaved PARP, an apoptosis marker, while it inhibited AKT in H358R cells (Figure 3d). These results suggest that iMDK induces apoptosis in sotorasib-resistant H358R cells through the induction of ATF3-mediated apoptosis but not by the PI3K-AKT pathway inhibition (Figure 3e).

iMDK Encapsulated in Lipid Nanoparticles (LNP; DPPC/DOTAP/DSPE-PEG/Cholesterol) Being Soluble in Water and Inducing Apoptosis in H441 Cells In Vitro. Due to its hydrophobic structure (Figure 1a), iMDK is not soluble in water, which hampers efforts to translate iMDK into the clinic. To make iMDK soluble in water, we employed nanoparticles that can encapsulate hydrophobic small molecules in the hydrophobic inner layer. The iMDK encapsulated in the LNP is soluble in water in theory due to the hydrophilic outside surface of the LNP. We tested three water-soluble nanoparticles (lipid or polymer) as possible vehicles for encapsulating and delivering iMDK in water: (1) DPPC/DOTAP/DSPE-PEG/Cholesterol (lipid), (2) DPPC/DPPG/DSPE-PEG/Cholesterol (lipid), and (3) PEI−PEG-LinA (polymer). We mixed iMDK dissolved in tetrahydrofuran (THF), an organic solvent, with these three different nanoparticles dissolved in water. THF was removed from iMDK-nanoparticle mixtures with an evaporator followed by dialysis in water (Figure 4a,b), as described in the Methods section. We measured the surface charges and sizes of these iMDK-encapsulating nanoparticles in water using a Zetasizer since positively charged and uniformly distributed nanoparticles are required to deliver small molecules efficiently into cancer cells.[20] The surface charges of DPPC/DOTAP/DSPE-PEG/Cholesterol (hereafter, LNP[DOTAP]), DPPC/DPPG/DSPE-PEG/Cholesterol (hereafter, LNP[DPPG]), and PEI−PEG-LinA were 28, −20.9, and 32 mV, respectively (Figure 4c), indicating that LNP[DOTAP] and PEI−PEG-LinA are positively charged while LNP[DPPG] is negatively charged. The size distribution of LNP[DOTAP] and LNP[DPPG] was uniformly distributed around 200 nm, while that of PEI−PEG-LinA was not uniformly distributed around 400 nm (Figure 4d). We then treated H441 cells with these three different nanoparticle formulations encapsulating iMDK and assessed cell viability, the ATF3-CHOP pathway, and PI3K-AKT pathway activities. Notably, LNP[DOTAP] containing iMDK significantly inhibited cell viability associated with induction of the ATF3-CHOP pathway and inhibition of the PI3K-AKT pathway in H441 cells, while the other nanoparticles, LNP[DPPG] and PEI−PEG-LinA, did not (Figure 4e,f), indicating that water-soluble LNP[DOTAP] is suitable to deliver iMDK into H441 cells in vitro.

DPPC/DOTAP/DSPE-PEG/Cholesterol Nanoparticles (LNP[DOTAP]) Encapsulating iMDK Suppress the Growth of H441 Cell Xenografts In Vivo. To assess whether water-soluble LNP[DOTAP] (hereafter, LNP) that encapsulates iMDK (iMDK-LNP) suppresses growth of H441 cells in vivo, we established an H441 xenograft model using nude mice and treated one group of mice by intraperitoneal (IP) injection with iMDK-LNP and the other group of mice

https://doi.org/10.1021/acs.molpharmaceut.5c00550
Mol. Pharmaceutics XXXX, XXX, XXX−XXX

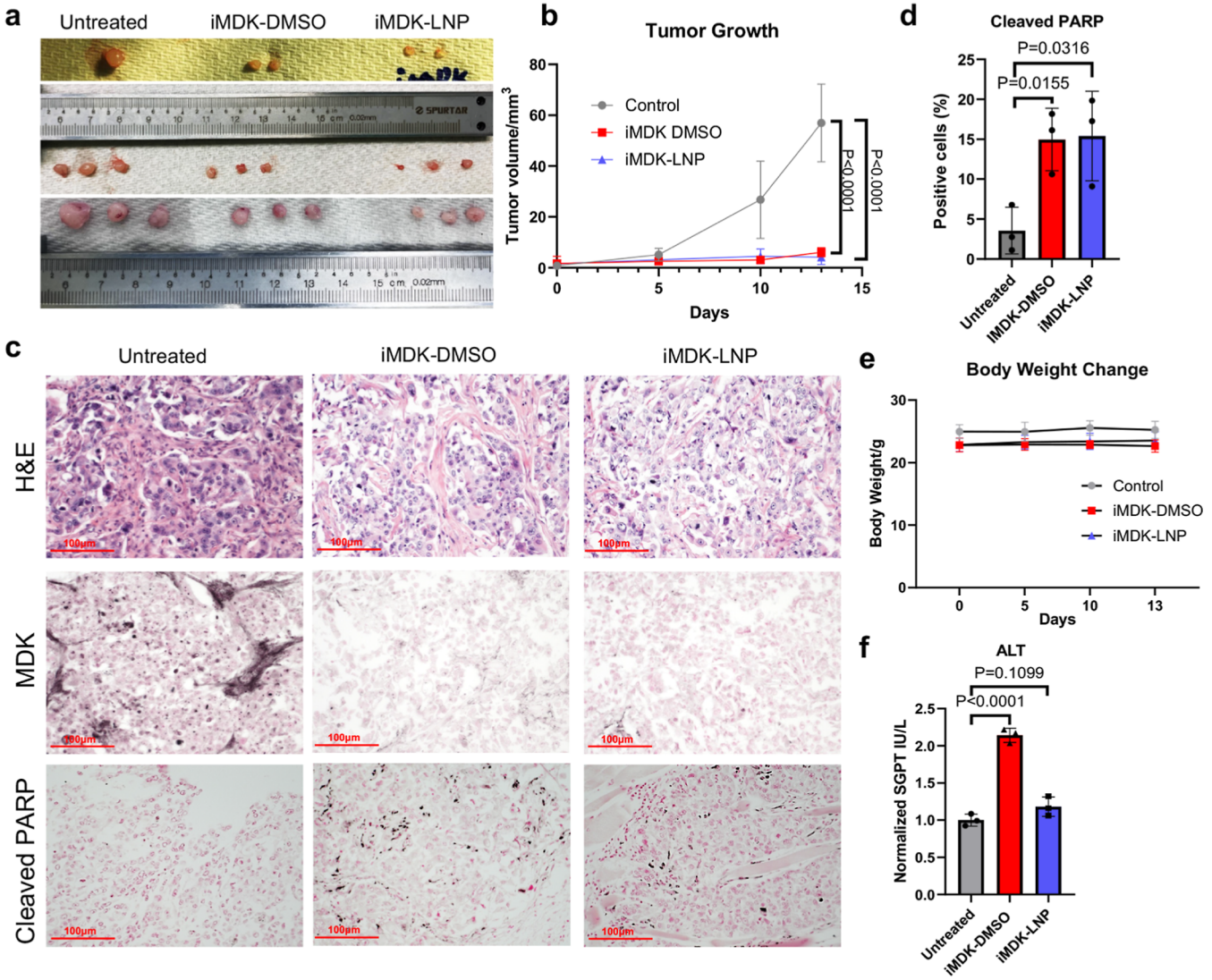

Figure 5. Lipid nanoparticles (LNP; DPPC/DOTAP/DSPE-PEG/Cholesterol) carrying iMDK (iMDK-LNP) induce apoptosis in H441 xenografts without causing liver toxicity. (a) Shown are H441 xenografts from nude mice that were intraperitoneally treated with iMDK dissolved in DMSO (iMDK-DMSO) or iMDK-LNP at 9.7 mg/kg body weight once daily for 13 days. (b) Tumor volume of H441 xenografts that were untreated (n = 7) or treated with iMDK-DMSO (n = 8) or iMDK-LNP (n = 8), as described in (a). P values comparing day-13 tumor volumes are shown. (c) Morphology and the expression of MDK and cleaved PARP in H441 xenografts from (a,b) are shown by H&E and immunohistochemical staining. Bars = 100 μm. (d) Cleaved PARP1-positive cells (%) in H441 xenografts from (c) (n = 3). (e) Body weight of nude mice with H441 xenografts described in (b). (f) ALT activity from serum of nude mice with H441 xenografts that were untreated or treated with iMDK-DMSO or iMDK-LNP as described in (a) for 13 days (n = 3). All P values are from Student's t-test, as indicated. Error bars represent ± standard deviation.

with iMDK dissolved in DMSO (iMDK-DMSO). Notably, iMDK-DMSO and iMDK-LNP significantly suppressed the growth of H441 xenografts in both groups compared with untreated H441 xenografts (Figure 5a,b). MDK protein expression in H441 xenografts from iMDK-DMSO or iMDK-LNP treated mice was reduced compared with that from untreated mice (Figure 5c). Cleaved PARP was significantly induced in H441 xenografts from iMDK-DMSO- or iMDK-LNP-treated mice compared to that from untreated mice (Figure 5c,d). Importantly, body weight was not affected in iMDK-DMSO-treated mice or iMDK-LNP-treated mice compared with untreated mice (Figure 5e). The activity of ALT, a marker for liver toxicity, was induced in iMDK-DMSO-treated mice but not in iMDK-LNP-treated mice compared to that in untreated mice (Figure 5f). These results indicate that IP-injected water-soluble iMDK-LNP is as effective as iMDK-DMSO for inducing apoptosis in H441 cells and is less toxic to the liver than iMDK-DMSO in vivo.

DISCUSSION

iMDK, which was originally identified as a small molecule that represses the expression of MDK, has been shown to suppress the growth of different types of cancers, including KRAS mutant lung cancers; however, the molecular mechanism by which iMDK suppresses the growth of cancer cells is not fully understood. Here, using RNA-seq combined with a CRISPR/Cas9-mediated gene knockout approach, we determined that iMDK suppresses the growth of H441 cells through the induction of the ATF3-CHOP-mediated apoptotic pathway. Using lipid nanoparticle technology, we also succeeded in dissolving hydrophobic iMDK in water by encapsulating

https://doi.org/10.1021/acs.molpharmaceut.5c00550
Mol. Pharmaceutics XXXX, XXX, XXX−XXX

iMDK in water-soluble lipid nanoparticles. iMDK in lipid nanoparticles (iMDK-LNP) was as efficient in inducing apoptosis in H441 cells as iMDK in DMSO (iMDK-DMSO), while iMDK-LNP did not cause liver toxicity compared to iMDK-DMSO. Our data indicate that iMDK-LNP is a promising and translatable anticancer drug to target subsets of lung cancers that harbor mutant KRAS.

Activation of the ER stress pathway has been considered as a promising approach to tumor growth suppression for the past two decades.[21,22] For example, an FDA-approved drug, bortezomib, that activates the ER stress pathway to induce apoptosis has been used to treat multiple myeloma and mantle cell lymphoma.[23] Induction of ATF3 was shown to be critical for bortezomib-mediated apoptosis in multiple myeloma,[24] consistent with our data that ATF3 is required for iMDK-mediated apoptosis in H441 papillary lung adenocarcinoma cells. Since iMDK was also shown to induce apoptosis in multiple myeloma cell lines,[6] it would be worth determining whether iMDK-mediated apoptosis in multiple myeloma is also through the activation of the ATF3-CHOP ER stress pathway. Bortezomib was previously reported to induce apoptosis in A549 cells more efficiently than in H441 cells[25] in contrast to our finding that iMDK induces apoptosis in H441 cells but not A549 cells, suggesting that the mechanism of action on ER-mediated apoptosis by iMDK is different from that of bortezomib. This also suggests that iMDK might be useful in treating bortezomib-resistant multiple myeloma.

Although we focused on the ATF3-CHOP ER stress pathway in the present study, our RNA-seq analysis indicated that other ER stress response genes such as PERK/EIF2AK3, IRE1alpha/ERN1, and TRB3/TRIB3[17] were also induced by iMDK in H441 cells (Tables S1 and S3). Such other ER stress genes might be critical for iMDK-mediated apoptosis in H441 cells, which can be validated by the CRISPR/Cas9-mediated knockout approach used in this study. Since *TNF* was induced in both iMDK-sensitive H441 cells and iMDK-resistant A549 cells, we did not focus on the role of TNF; however, further validation using the knockout approach for TNF would determine the definitive role of TNF in iMDK-mediated apoptosis in H441 cells. Of note, mRNA of ATF4, which is another ER stress gene,[17] was not highly induced by iMDK (<1.5 fold: Table S3), which might be because the nuclear translocation of ATF4 protein but not the induction of ATF4 mRNA is critical upon ER stress. TRB3/TRIB3, a downstream gene of CHOP,[17,26] is known to prevent AKT phosphorylation,[17,27] which suggests that the increase of AKT phosphorylation in ATF3 or CHOP knockout H441 cells seen in our study (Figure 2) might be through the decreased TRB3/TRIB3 in such knockout H441 cells. However, the roles of ATF4 and TRB3/TRIB3 in iMDK-mediated apoptosis need to be validated at the protein level along with the knockout approach in the future.

Therapy for unresectable lung adenocarcinomas has been revolutionized in part thanks to small molecules that bind to mutant driver oncogenes, including mutant KRAS, and suppress tumor growth.[28] Unfortunately, most lung adenocarcinomas that initially respond to such small molecules recur later, suggesting that a subsequent approach to treat recurrent lung adenocarcinomas is critically needed. For example, the recent discovery of small molecule inhibitors (e.g., sotorasib) that bind to $KRAS^{G12C}$ has revolutionized the treatment of patients with lung cancer that harbor $KRAS^{G12C}$; however, recurrence by different molecular mechanisms is most likely.[8] One of the recurrence mechanisms is the activation of the PI3K-AKT pathway, which enables cancer cells that harbor $KRAS^{G12C}$ to evade $KRAS^{G12C}$ inhibition.[29,30] PI3K-AKT inhibitors were shown to suppress the growth of a subset of sotorasib-resistant cell lines that harbor $KRAS^{G12C}$;[29,30] however, miransertib,[14] a PI3K-AKT inhibitor, failed to induce apoptosis in sotorasib-resistant H358R cells that carry $KRAS^{G12C}$ (Figures 1 and 3), indicating that inhibition of the PI3K-AKT pathway is not sufficient to suppress the growth of a portion of $KRAS^{G12C}$ inhibitor-resistant cancer cells. In the present study, we demonstrated that iMDK inhibited the PI3K-AKT pathway, induced ATF3, and caused apoptosis in sotorasib-resistant H358R cells that carry $KRAS^{G12C}$. The lack of CHOP induction by iMDK in H358R cells suggests that ATF3 induced by iMDK may also mediate apoptosis through a CHOP-independent pathway (e.g., NOXA/PMAIP1), the potential mechanism of which is supported by clinical data indicating that the induction of *ATF3* but not CHOP was significantly associated with longer progression-free survival upon bortezomib plus dexamethasone therapy.[24,31] Thus, iMDK performs better than PI3K-AKT pathway inhibitors and warrants further studies of iMDK for translation into the clinic.

In the present study, we succeeded in encapsulating water-insoluble iMDK into the water-soluble lipid nanoparticle DPPC/DOTAP/DSPE-PEG/Cholesterol (LNP[DOTAP]) to deliver iMDK intraperitoneally into H441 xenografts without liver toxicity in vivo. This approach has been previously used to enable the hydrophobic small molecule paclitaxel to be administered in water by using albumin-bound nanoparticles. This achievement resulted in nab-paclitaxel (also known as Abraxane), an FDA-approved-paclitaxel derived drug for treating lung and breast cancers with reduced side toxicity compared to paclitaxel dissolved in polyoxyethylated castor oil (Cremophor EL) and ethanol.[32] To the best of our knowledge, our lipid nanoparticle composition has not been used for encapsulating any hydrophobic small molecules, including iMDK, for preclinical and clinical studies. Although the physical and/or serum stability of our lipid nanoparticles needs to be investigated, Gangurde et al. have shown that PEG helps to create uniform lipid nanoparticles while DOTAP and cholesterol destabilize and stabilize lipid nanoparticles, respectively, for cationic light-activated liposomes.[33] For hydrophobic small molecules that are not eligible for albumin-bound nanoparticles, our lipid nanoparticle composition might be useful to deliver such molecules in vivo. However, further pharmacokinetics, pharmacodynamics, and toxicity studies, not only for the liver but also the kidney and other organs, in larger animals will be necessary in the future.

CONCLUSIONS

Our study indicates that iMDK encapsulated in lipid nanoparticles can be administered to mice with less side toxicity than DMSO. We have shown that iMDK induces ATF3-mediated apoptosis in subsets of human KRAS mutant lung cancer cells, including $KRAS^{G12C}$ inhibitor-resistant lung cancer cells that do not respond to a PI3K-AKT inhibitor, which suggests that iMDK is a promising therapeutic candidate for treatment of KRAS inhibitor-resistant cancers.

https://doi.org/10.1021/acs.molpharmaceut.5c00550
Mol. Pharmaceutics XXXX, XXX, XXX−XXX

■ ASSOCIATED CONTENT

Supporting Information

The Supporting Information is available free of charge at https://pubs.acs.org/doi/10.1021/acs.molpharmaceut.5c00550.

RNA-seq and raw data (XLSX)
Whole immunoblot images (PDF)

■ AUTHOR INFORMATION

Corresponding Author

Yutaka Maeda − *Perinatal Institute, Division of Neonatology, Perinatal and Pulmonary Biology, The University of Cincinnati College of Medicine, Cincinnati, Ohio 45229-3039, United States;* orcid.org/0000-0002-9537-3971; Phone: +1-513-803-5066; Email: yutaka.maeda@cchmc.org; Fax: +1-513-636-7868

Authors

Bingxin Liu − *Perinatal Institute, Division of Neonatology, Perinatal and Pulmonary Biology, The University of Cincinnati College of Medicine, Cincinnati, Ohio 45229-3039, United States; The Materials Science and Engineering Program, Department of Mechanical and Materials Engineering, The University of Cincinnati College of Medicine, Cincinnati, Ohio 45229, United States*

Iris M. Fink-Baldauf − *Perinatal Institute, Division of Neonatology, Perinatal and Pulmonary Biology, The University of Cincinnati College of Medicine, Cincinnati, Ohio 45229-3039, United States*

William D. Stuart − *Perinatal Institute, Division of Neonatology, Perinatal and Pulmonary Biology, The University of Cincinnati College of Medicine, Cincinnati, Ohio 45229-3039, United States*

Cheng Jiang − *Perinatal Institute, Division of Neonatology, Perinatal and Pulmonary Biology, The University of Cincinnati College of Medicine, Cincinnati, Ohio 45229-3039, United States*

Anjaparavanda P. Naren − *Division of Pulmonary Medicine, Cincinnati Children's Hospital Medical Center (CCHMC) and Department of Pediatrics, The University of Cincinnati College of Medicine, Cincinnati, Ohio 45229-3039, United States;* Present Address: Division of Pulmonary Medicine and Critical Care, Cedars-Sinai Medical Center, Los Angeles, California, United States

Donglu Shi − *The Materials Science and Engineering Program, Department of Mechanical and Materials Engineering, The University of Cincinnati College of Medicine, Cincinnati, Ohio 45229, United States*

Minzhe Guo − *Perinatal Institute, Division of Neonatology, Perinatal and Pulmonary Biology, The University of Cincinnati College of Medicine, Cincinnati, Ohio 45229-3039, United States*

Jeffrey A. Whitsett − *Perinatal Institute, Division of Neonatology, Perinatal and Pulmonary Biology, The University of Cincinnati College of Medicine, Cincinnati, Ohio 45229-3039, United States*

Complete contact information is available at: https://pubs.acs.org/10.1021/acs.molpharmaceut.5c00550

Author Contributions

B.L., A.P.N., and Y.M. conceptualized and designed the study. B.L., I.M.F.-B., W.D.S., C.J., M.G., and Y.M. conducted the investigation. D.S., J.A.W., and Y.M. supervised the work. B.L. and Y.M. wrote the original draft. B.L., W.D.S., J.A.W., and Y.M. revised and edited the manuscript.

Notes

The authors declare the following competing financial interest(s): The authors filed an invention disclosure for the lipid nanoparticle.

■ ACKNOWLEDGMENTS

This work was supported by NIH grants (U01HL134745, U01HL148856, R01HL164414, R01CA240317, R01HL147351, and P30DK117467), University of Cincinnati Cancer Center grants (S323349-2023 Ride Cincinnati-Maeda, the Bergman Family Lung Cancer Research Fund, and the Tim Kimmel Family Lung Cancer Research Fund and TAM Award), and the Cincinnati Children's Hospital Medical Center (CF-RDP Pilot & Feasibility Grant). We thank Jaymi St. Arnold and Mary Durbin for assistance and discussions.

■ REFERENCES

(1) Hao, H.; Maeda, Y.; Fukazawa, T.; Yamatsuji, T.; Takaoka, M.; Bao, X. H.; Matsuoka, J.; Okui, T.; Shimo, T.; Takigawa, N.; Tomono, Y.; Nakajima, M.; Fink-Baldauf, I. M.; Nelson, S.; Seibel, W.; Papoian, R.; Whitsett, J. A.; Naomoto, Y. Inhibition of the growth factor MDK/midkine by a novel small molecule compound to treat non-small cell lung cancer. *PLoS One* **2013**, *8* (8), No. e71093.

(2) Masui, M.; Okui, T.; Shimo, T.; Takabatake, K.; Fukazawa, T.; Matsumoto, K.; Kurio, N.; Ibaragi, S.; Naomoto, Y.; Nagatsuka, H.; Sasaki, A. Novel Midkine Inhibitor iMDK Inhibits Tumor Growth and Angiogenesis in Oral Squamous Cell Carcinoma. *Anticancer Res.* **2016**, *36* (6), 2775−2781.

(3) Erdogan, S.; Doganlar, Z. B.; Doganlar, O.; Turkekul, K.; Serttas, R. Inhibition of Midkine Suppresses Prostate Cancer CD133^{+} Stem Cell Growth and Migration. *Am. J. Med. Sci.* **2017**, *354* (3), 299−309.

(4) Shin, D. H.; Jo, J. Y.; Kim, S. H.; Choi, M.; Han, C.; Choi, B. K.; Kim, S. S. Midkine Is a Potential Therapeutic Target of Tumorigenesis, Angiogenesis, and Metastasis in Non-Small Cell Lung Cancer. *Cancers* **2020**, *12* (9), 2402.

(5) Ueno, M.; Kariya, R.; Gunya, S.; Cheevapruk, K.; Okada, S. Midkine inhibitor (iMDK) induces apoptosis of primary effusion lymphoma via G2/M cell cycle arrest. *Leuk. Res.* **2022**, *116*, 106826.

(6) Cheevapruk, K.; Ueno, M.; Sungwan, P.; Sittithumcharee, G.; Kariya, R.; Sampattavanich, S.; Okada, S. Novel Midkine Inhibitor Induces Cell Cycle Arrest and Apoptosis in Multiple Myeloma. *Anticancer Res.* **2024**, *44* (3), 1023−1031.

(7) Ishida, N.; Fukazawa, T.; Maeda, Y.; Yamatsuji, T.; Kato, K.; Matsumoto, K.; Shimo, T.; Takigawa, N.; Whitsett, J. A.; Naomoto, Y. A novel PI3K inhibitor iMDK suppresses non-small cell lung Cancer cooperatively with A MEK inhibitor. *Exp. Cell Res.* **2015**, *335* (2), 197−206.

(8) Awad, M. M.; Liu, S.; Rybkin, I. I.; Arbour, K. C.; Dilly, J.; Zhu, V. W.; Johnson, M. L.; Heist, R. S.; Patil, T.; Riely, G. J.; Jacobson, J. O.; Yang, X.; Persky, N. S.; Root, D. E.; Lowder, K. E.; Feng, H.; Zhang, S. S.; Haigis, K. M.; Hung, Y. P.; Sholl, L. M.; Wolpin, B. M.; Wiese, J.; Christiansen, J.; Lee, J.; Schrock, A. B.; Lim, L. P.; Garg, K.; Li, M.; Engstrom, L. D.; Waters, L.; Lawson, J. D.; Olson, P.; Lito, P.; Ou, S. I.; Christensen, J. G.; Jänne, P. A.; Aguirre, A. J. Acquired Resistance to KRAS^{G12C} Inhibition in Cancer. *N. Engl. J. Med.* **2021**, *384* (25), 2382−2393.

(9) Zhao, Y.; Murciano-Goroff, Y. R.; Xue, J. Y.; Ang, A.; Lucas, J.; Mai, T. T.; Da Cruz Paula, A. F.; Saiki, A. Y.; Mohn, D.; Achanta, P.; Sisk, A. E.; Arora, K. S.; Roy, R. S.; Kim, D.; Li, C.; Lim, L. P.; Li, M.; Bahr, A.; Loomis, B. R.; de Stanchina, E.; Reis-Filho, J. S.; Weigelt, B.; Berger, M.; Riely, G.; Arbour, K. C.; Lipford, J. R.; Li, B. T.; Lito, P. Diverse alterations associated with resistance to KRAS(G12C) inhibition. *Nature* **2021**, *599* (7886), 679−683.

(10) Tomoshige, K.; Stuart, W. D.; Fink-Baldauf, I. M.; Ito, M.; Tsuchiya, T.; Nagayasu, T.; Yamatsuji, T.; Okada, M.; Fukazawa, T.; Guo, M.; Maeda, Y. FOXA2 Cooperates with Mutant KRAS to Drive Invasive Mucinous Adenocarcinoma of the Lung. *Cancer Res.* **2023**, *83* (9), 1443−1458.
(11) Love, M. I.; Huber, W.; Anders, S. Moderated estimation of fold change and dispersion for RNA-seq data with DESeq2. *Genome Biol.* **2014**, *15* (12), 550.
(12) Chen, J.; Bardes, E. E.; Aronow, B. J.; Jegga, A. G. ToppGene Suite for gene list enrichment analysis and candidate gene prioritization. *Nucleic Acids Res.* **2009**, *37*, W305−W311.
(13) Dunn, A. W.; Kalinichenko, V. V.; Shi, D. Highly Efficient In Vivo Targeting of the Pulmonary Endothelium Using Novel Modifications of Polyethylenimine: An Importance of Charge. *Adv. Healthc Mater.* **2018**, *7* (23), No. e1800876.
(14) Lapierre, J. M.; Eathiraj, S.; Vensel, D.; Liu, Y.; Bull, C. O.; Cornell-Kennon, S.; Iimura, S.; Kelleher, E. W.; Kizer, D. E.; Koerner, S.; Makhija, S.; Matsuda, A.; Moussa, M.; Namdev, N.; Savage, R. E.; Szwaya, J.; Volckova, E.; Westlund, N.; Wu, H.; Schwartz, B. Discovery of 3-(3-(4-(1-Aminocyclobutyl)phenyl)-5-phenyl-3H-imidazo[4,5-b]pyridin-2-yl)pyridin-2-amine (ARQ 092): An Orally Bioavailable, Selective, and Potent Allosteric AKT Inhibitor. *J. Med. Chem.* **2016**, *59* (13), 6455−6469.
(15) Jiang, H. Y.; Wek, S. A.; McGrath, B. C.; Lu, D.; Hai, T.; Harding, H. P.; Wang, X.; Ron, D.; Cavener, D. R.; Wek, R. C. Activating transcription factor 3 is integral to the eukaryotic initiation factor 2 kinase stress response. *Mol. Cell. Biol.* **2004**, *24* (3), 1365−1377.
(16) Liu, Z.; Shi, Q.; Song, X.; Wang, Y.; Wang, Y.; Song, E.; Song, Y. Activating Transcription Factor 4 (ATF4)-ATF3-C/EBP Homologous Protein (CHOP) Cascade Shows an Essential Role in the ER Stress-Induced Sensitization of Tetrachlorobenzoquinone-Challenged PC12 Cells to ROS-Mediated Apoptosis via Death Receptor 5 (DR5) Signaling. *Chem. Res. Toxicol.* **2016**, *29* (9), 1510−1518.
(17) Hu, H.; Tian, M.; Ding, C.; Yu, S. The C/EBP Homologous Protein (CHOP) Transcription Factor Functions in Endoplasmic Reticulum Stress-Induced Apoptosis and Microbial Infection. *Front. Immunol.* **2019**, *9*, 3083.
(18) Micheau, O.; Tschopp, J. Induction of TNF receptor I-mediated apoptosis via two sequential signaling complexes. *Cell* **2003**, *114* (2), 181−190.
(19) Nakajima, E. C.; Drezner, N.; Li, X.; Mishra-Kalyani, P. S.; Liu, Y.; Zhao, H.; Bi, Y.; Liu, J.; Rahman, A.; Wearne, E.; Ojofeitimi, I.; Hotaki, L. T.; Spillman, D.; Pazdur, R.; Beaver, J. A.; Singh, H. FDA Approval Summary: Sotorasib for KRAS G12C-Mutated Metastatic NSCLC. *Clin. Cancer Res.* **2022**, *28* (8), 1482−1486.
(20) Verma, A.; Stellacci, F. Effect of surface properties on nanoparticle-cell interactions. *Small* **2010**, *6* (1), 12−21.
(21) Kim, I.; Xu, W.; Reed, J. C. Cell death and endoplasmic reticulum stress: disease relevance and therapeutic opportunities. *Nat. Rev. Drug Discovery* **2008**, *7* (12), 1013−1030.
(22) Schönthal, A. H. Pharmacological targeting of endoplasmic reticulum stress signaling in cancer. *Biochem. Pharmacol.* **2013**, *85* (5), 653−666.
(23) Richardson, P. G.; Sonneveld, P.; Schuster, M. W.; Irwin, D.; Stadtmauer, E. A.; Facon, T.; Harousseau, J. L.; Ben-Yehuda, D.; Lonial, S.; Goldschmidt, H.; Reece, D.; San-Miguel, J. F.; Bladé, J.; Boccadoro, M.; Cavenagh, J.; Dalton, W. S.; Boral, A. L.; Esseltine, D. L.; Porter, J. B.; Schenkein, D.; Anderson, K. C. Assessment of Proteasome Inhibition for Extending Remissions (APEX) Investigators. Bortezomib or high-dose dexamethasone for relapsed multiple myeloma. *N. Engl. J. Med.* **2005**, *352* (24), 2487−2498.
(24) Narita, T.; Ri, M.; Masaki, A.; Mori, F.; Ito, A.; Kusumoto, S.; Ishida, T.; Komatsu, H.; Iida, S. Lower expression of activating transcription factors 3 and 4 correlates with shorter progression-free survival in multiple myeloma patients receiving bortezomib plus dexamethasone therapy. *Blood Cancer J.* **2015**, *5* (12), No. e373.
(25) Li, Y.; Dong, S.; Tamaskar, A.; Wang, H.; Zhao, J.; Ma, H.; Zhao, Y. Proteasome Inhibitors Diminish c-Met Expression and Induce Cell Death in Non-Small Cell Lung Cancer Cells. *Oncol. Res.* **2020**, *28* (5), 497−507.
(26) Ohoka, N.; Yoshii, S.; Hattori, T.; Onozaki, K.; Hayashi, H. TRB3, a novel ER stress-inducible gene, is induced via ATF4-CHOP pathway and is involved in cell death. *EMBO J.* **2005**, *24* (6), 1243−1255.
(27) Du, K.; Herzig, S.; Kulkarni, R. N.; Montminy, M. TRB3: a tribbles homolog that inhibits Akt/PKB activation by insulin in liver. *Science* **2003**, *300* (5625), 1574−1577.
(28) Tan, A. C.; Tan, D. S. W. Targeted Therapies for Lung Cancer Patients With Oncogenic Driver Molecular Alterations. *J. Clin. Oncol.* **2022**, *40* (6), 611−625.
(29) Misale, S.; Fatherree, J. P.; Cortez, E.; Li, C.; Bilton, S.; Timonina, D.; Myers, D. T.; Lee, D.; Gomez-Caraballo, M.; Greenberg, M.; Nangia, V.; Greninger, P.; Egan, R. K.; McClanaghan, J.; Stein, G. T.; Murchie, E.; Zarrinkar, P. P.; Janes, M. R.; Li, L. S.; Liu, Y.; Hata, A. N.; Benes, C. H. KRAS G12C NSCLC Models Are Sensitive to Direct Targeting of KRAS in Combination with PI3K Inhibition. *Clin. Cancer Res.* **2019**, *25* (2), 796−807.
(30) Chan, C. H.; Chiou, L. W.; Lee, T. Y.; Liu, Y. R.; Hsieh, T. H.; Yang, C. Y.; Jeng, Y. M. PAK and PI3K pathway activation confers resistance to $KRAS^{G12C}$ inhibitor sotorasib. *Br. J. Cancer* **2023**, *128* (1), 148−159.
(31) Edagawa, M.; Kawauchi, J.; Hirata, M.; Goshima, H.; Inoue, M.; Okamoto, T.; Murakami, A.; Maehara, Y.; Kitajima, S. Role of activating transcription factor 3 (ATF3) in endoplasmic reticulum (ER) stress-induced sensitization of p53-deficient human colon cancer cells to tumor necrosis factor (TNF)-related apoptosis-inducing ligand (TRAIL)-mediated apoptosis through up-regulation of death receptor 5 (DR5) by zerumbone and celecoxib. *J. Biol. Chem.* **2014**, *289* (31), 21544−21561.
(32) Ma, P.; Mumper, R. J. Paclitaxel Nano-Delivery Systems: A Comprehensive Review. *J. Nanomed. Nanotechnol.* **2013**, *4* (2), 1000164.
(33) Gangurde, P.; Mahmoudzadeh, M.; Gounani, Z.; Koivuniemi, A.; Laurén, P.; Lajunen, T.; Laaksonen, T. Development of Robust Cationic Light-Activated Thermosensitive Liposomes: Choosing the Right Lipids. *Mol. Pharmaceutics* **2023**, *20* (11), 5728−5738.

https://doi.org/10.1021/acs.molpharmaceut.5c00550
Mol. Pharmaceutics XXXX, XXX, XXX−XXX